Submitted to: 81st SEG Annual Meeting, San Antonio, 2011

3D geology, temperature, heat flow and thermal gradient modeling of the north Perth Basin, Western Australia

Helen Gibson, Ray Seikel and Desmond FitzGerald Intrepid Geophysics; Mike Middleton and Ameed Ghori, Department of Mines and Petroleum Western Australia*

Summary

Aiming to achieve an accurate steady state, 3D conductive heat flow model of the north Perth Basin, we first built a well-constrained 3D geology model and compiled best-available thermal conductivity and heat production rate data. A finite difference code implemented in the same software (*3D GeoModeller*) enabled computation of 3D temperatures, heat flows, and geothermal gradients directly from the geology model.

As well as direct visualization of the resulting 3D grids, we derived 2D grids including: i) temperature-maps of chosen depth horizons; ii) depth-maps of chosen isotherm surfaces; iii) a surface heat flow grid (draped to fit topography); and iv) vertical and horizontal temperature gradient-maps for chosen depth slices.

This study has implications for geothermal energy exploration in Western Australia where the search for Enhanced Geothermal Systems (EGS) or direct-use heat plays begins with identification of anomalously high heat occurrences at accessibly shallow depths.

Introduction

The Perth Basin is located onshore, north of Perth, parallel to the West Australian coast, between the latitudes of 27°S and 34°30'S (Fig. 2). It is an NNW to SSE trending elongate rift basin lying between the Yilgarn Block to the east, and the edge of the continental shelf to the west (Mory et al. 2005). Basement comprises Pre-Cambrian gneisses of the Pinjarra Orogen which outcrop as fault-bounded, mid-basin ridges. These deep structures were most recently reactivated by the Darling Fault which is integral to the architecture of the Perth Basin (Fitzsimons 2002).

The Perth Basin formed during separation of Australia and Greater India in the Permian to Early Cretaceous, and thus contains predominantly Early Permian to Late Cretaceous sedimentary sequences up to 15 km thick (Freeman and Donaldson, 2006).

Building the geology model

Our geology model of the north Perth Basin (x=142km; y=280km; z=16km) was built using diverse geologic data to implicitly guide the 3D interpolators. Interpolation adopted a potential field method (Lajaunie et al. 1997), and thus honoured both geology contact and orientation data in building 3D shapes of each geological unit.

Constraints of the geology model include:

- Formation-tops data from 96 petroleum and stratigraphic drill holes;
- Digitized contacts from geology cross-sections: A-A' to G-G' (from Mory & Iasky 1996, devised from drilling and seismic survey results);
- Digitized contacts from a pre-Cainozoic Geology Map (plate 10, Mory & Iasky 1996);
- Digitized contacts from a geology map compiled by M. Sandiford (in Mory et. al. 2005) – for modelling the far north region.
- Digitized contacts from a tectonic divisions map, northern Perth Basin compiled by M. Sandiford (from Mory et al 2005) – for modelling offshore structures.
- A depth to basement grid (.xyz) digitized from a contoured top-basement depth structure map (plate 5, Mory & Iasky 1996).

Rule-based modeling was applied, so that the arrangement of the stratigraphic pile (Fig. 1) and the fault relationships (Fig. 2) also constrained the model.

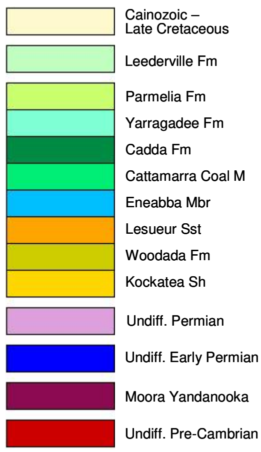

Figure 1: Stratigraphy of the north Perth Basin used to build the geology model. Note grouped units of the basin-fill are modeled with a single interpolator, while each unit separate within the pile, is modeled with an independent interpolator.

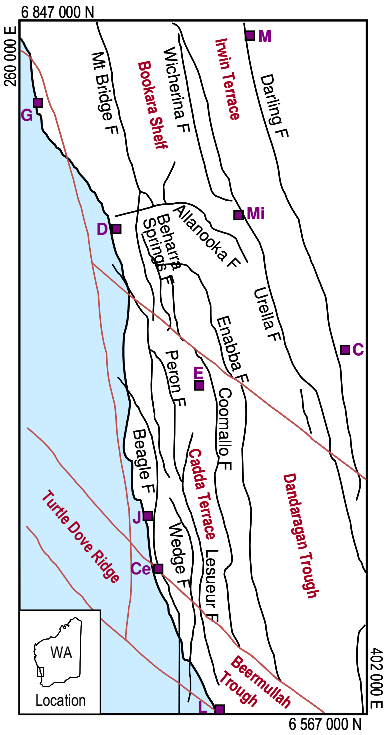

Figure 2: Location, structural elements and fault trace map of the north Perth Basin, Western Australia. [M= Mullewa; G=Geraldton; Mi=Mingenew; D=Dongara; C=Carnamah; E=Eneabba; J=Jurien; Ce=Cervantes; L=Lancelin.]

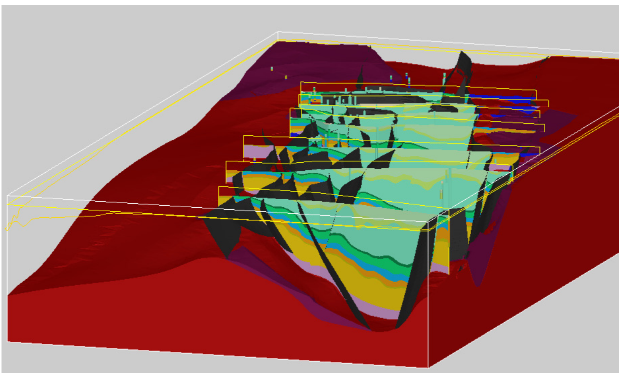

Figure 3: Oblique 3D view of the northern Perth Basin (from the south-east). Vertical exaggeration 3:1. This composite model presents solid volumes of Pre-Cambrian basement gneisses, rendered 2D sections of the Permian to Late Cretaceous basin sequences, modelled fault surfaces and exaggerated views of well intercepts (well radii 350m).

Verification of the resulting 3D geology model indicated all constraining geologic data were honoured, and that highly reasonable predictions of lithology and structure occur throughout the model space (Fig. 3).

3D temperature modelling

Our equation (Seikel et al. 2009) solved for the steady state 3D temperature field under consideration of spatially variable thermal conductivities and heat production rates (Table 1). Heat transfer by advection was ignored for this application. This is unlikely to be a significant limitation due to the general absence of known aquifers and springs in the study region, with the possible exception of the far south-east project region near the Gillingarra bores (Middleton, 2010).

The solver utilizes a regular orthogonal, Cartesian 3D grid created by discretising the smooth 3D geology model. 3D temperature is solved by explicit finite difference approximation, using a Gauss-Seidel iteration scheme until the maximum number of set iterations has been performed, or the set maximum residual temperature threshold is met, whichever occurs first. One iteration is deemed to have occurred when a computation has occurred in every cell.

	Mean Thermal Conductivity (W m-1K-1)	Mean Heat Production Rate (µWm-3)
Cainozoic - Late Cretaceous	1.42	0
Leederville Formation	2.56	0
Parmelia Formation	2.58	0.5
Yarragadee Formation	3.54	0.5
Cadda Formation	4.14	0.5
Cattamarra Coal Measures	3.73	0.5
Eneabba Member	2.62	0.5
Lesueur Sandstone	3.56	0.5
Woodada Formation	3.2	2.838
Kockatea Shale	2.09	0.5
Undifferentiated Permian	2.585	0.5
Undifferentiated Early Permian	2.299	0.5
Moora-Yandanooka Groups	3.2	2.838
Undifferentiated Pre-Cambrian	3.2	2.838

Table 1: Selected mean thermal rock property values for each lithology in the 3D geology model.

Calibration of suitable boundary conditions for the north Perth Basin model was achieved within 4 runs at low resolution (Table 2). Early run-results were verified against 28 down hole temperatures held fixed during convergence.

The final run was performed at high resolution (x=500m; y=500m; z=50m) representing discretization of the original model into ~51 million cells. The converged temperature solutions were written to a 3D grid, then further products were calculated including: vertical heat flow, and vertical and total horizontal temperature gradients (Table 3).

Boundary Conditions	Mean values for the nth Perth Basin model
Surface temperature	22°C (draped over topography) Adopted from the report by HDR 2008, this value was sourced from Australian Bureau of Meteorology data, and corrected upwards by 3°C, to account for surface rock insolation (as described by Howard and Sass, 1964).
Basal heat flow	0.049 μWm-2 Initially a value of 0.030 μWm-2 was used as appropriate for the steady state geotherm of continental lithosphere in the absence of radioactive heat production (Stuwe, 2007). This higher, final value is on par with some of the *lowest*, *surface* heat flow measurements in the north Perth Basin, as reported by HDR, 2008.
4 vertical sides	Neumann-type

Table 2: Boundary conditions for the final 3D temperature run.

3D temperature and other outputs	
Temperature	(°C) Solved for every cell centre by finite difference approximation.
Vertical heat flow	(Wm-2) Flow of heat measured in energy per time per unit area. Solved for each cell centre with respect to the centre of the cell immediately above.
Vertical temperature gradient	(°Ckm-1) Change of temperature over a distance. Solved for each cell centre with respect to the centre of the cell immediately above.
Total horizontal temperature gradient	(°Ckm-1) Change of temperature over a distance of one cell to 4 neighbours in the horizontal plane. Equal to the square root of the sum of the squares of the horizontal temperature gradients in the x and y directions. (An expression of gradient strength with no expression of direction within the horizontal plane.)

Table 3: Definitions and derivations of solved values for temperature, heat flow and geothermal gradients.

Results

3D results were computed at approximately 51 million cell centres within a 3D grid of identical extents and cell sizes to the discretized geological model for the north Perth Basin. In crude summary, the resulting temperature range for the project volume is 22 to 380°C.

Key findings show:

1. Five sites of relatively shallow, high temperature in the north Perth Basin – all generally located near sites with relatively shallow heat-producing basement, together with significant sedimentary cover (thermal insulator). See Table 4 and Fig. 4.

2. The 150°C isotherm surface spans depths from -3825 to -6670 m below sea level, which fluctuates from within and above basement. Temperatures of 150°C occur at depths shallower than 4 km, at five sites in the project area. (The same sites identified in Fig. 4.) See Fig. 5.

3. Significant areas of high modelled surface heat flow (Fig. 6) occur in areas of exposed basement (i.e. east of the Urella Fault, and on the Irwin Terrace and Bookara Shelf; Fig. 1). These are not generally co-incident with zones of high temperature anomalies. This is expected, because exposed or shallow basement rocks, without cover of thermally insulating sediments, loose heat effectively regardless of their typically higher internal heat production rates (compared with sediments).

4. Modelled vertical temperature gradients in the north Perth Basin are within normal ranges expected in typical crustal sections: 15 to 40°C/km. Gradients at the higher end of this range ~(40°C/km) generally occur at bounding edges between deep sedimentary troughs, and shallow basement zones. (See Fig 7). This general pattern (with lower magnitudes) is repeated in the results for total horizontal thermal gradients, not shown (see Gibson et al, 2010).

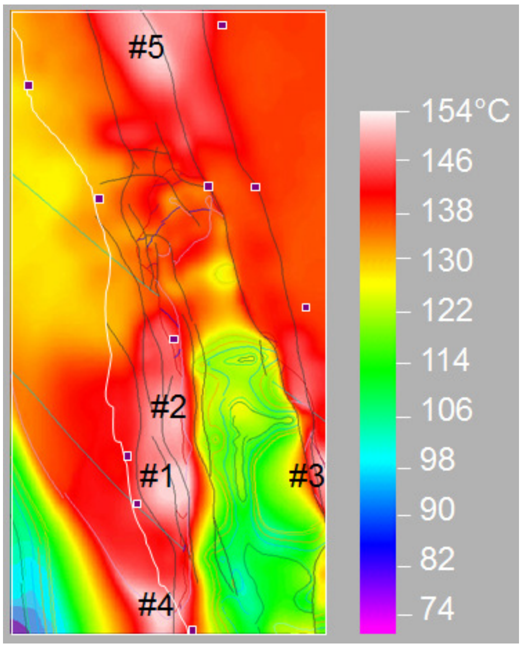

Figure 4: Plan view of computed 3D temperatures sliced through the -4000m level, together with the colour legend for the derived 2D grid (linear stretch). Locations of 5 high temperature anomalies (Table 4) are shown together with locations of faults and upper geology boundaries. Squares = town-locations from Fig. 1.

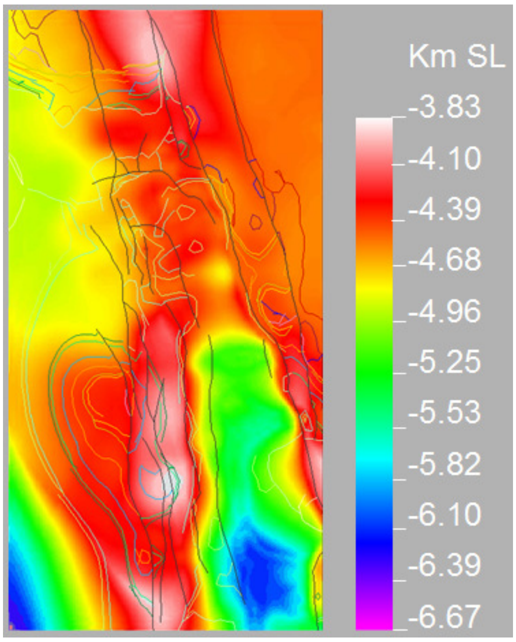

Figure 5: Derived 2D grid of depth to the 150°C isotherm (from the 3D voxet of temperatures), together with a colour legend for depth. The image is geo-located in the surface geology section to show the locations of fault traces (grey lines) and upper geology boundaries (colour legend from Fig. 1).

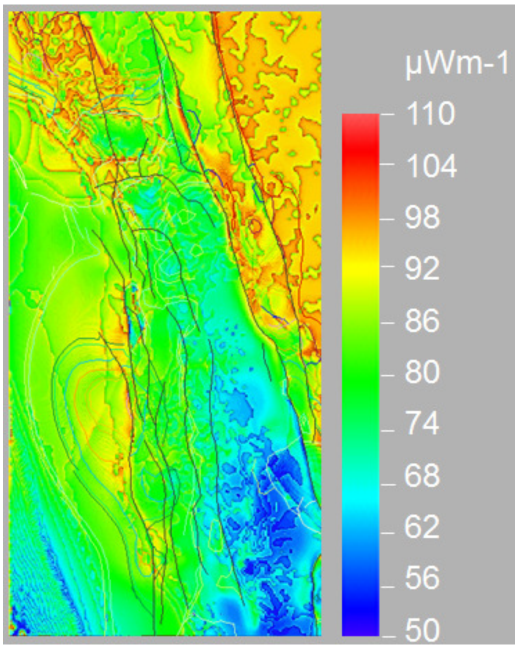

Figure 6: Image of the draped grid of modelled surface heat flow (μWm^{-2}) geo-located in the surface topography section to show the locations of faults (grey lines) and upper geology boundaries (from Fig. 1). The data range is clipped to exclude outliers. A linear stretch is applied to the colour legend of heat flow.

Temp. Anomaly	Approx. Easting	Approx. Northing	Landmark geology
#1	332 000	**6635 000**	Cadda Terrace
#2	332 000	6666 000	Cadda Terrace
#3	400 000	**6635 000**	east of Dandaragan Trough
#4	328 000	6576 000	Beermullah Trough
#5	325 000	6830 000	Bookara Shelf

Table 4: Approx. xy locations of high-temperature anomalies which are persistent at least between -2000 and -4000 m below SL.

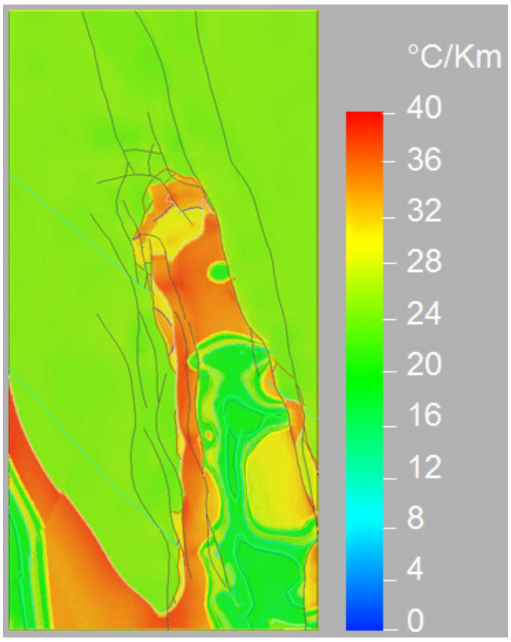

Figure 7: Modelled vertical temperature gradients (°C/Km) for the -4000m below SL section. The image is geo-located in the matching horizontal section of the geology model to show the locations of faults (grey lines) and geology boundaries.

Conclusions

Relatively high modelled temperatures occur in the north Perth Basin in areas containing relatively shallow basement (with internal heat production), together with a significant cover of sediments providing a thermal insulator.

Geology volumes and 3D distributions of thermal rock properties play a strong role influencing the spatial distributions of temperatures, thermal gradients and vertical heat flow. Therefore, modelling in 3D is crucial to obtaining accurate thermal predictions.

Acknowledgements

Intrepid Geophysics acknowledges the Department of Mines and Petroleum, Western Australia for its vision and funding to undertake this study.

REFERENCES

Fitzsimons I. C. W. 2002. Proterozoic basement provinces of southern and western Australia, and their correlation with Antarctica. *In* Proterozoic East Gondwana: Supercontinent Assembly and Breakup (eds.) Yoshida, M., Windley, B. F., and Dasgupta, S. 2002. Geol. Society Spec. Pub. No. 206.

Freeman, M. J., and Donaldson, M. J., 2006, Geology of the southern Perth Basin and Margaret River wine district, southwestern Western Australia — a field guide: Western Australia Geological Survey, Record 2006/20.

Hot Dry Rock Pty Ltd, 2008 Geothermal energy potential in selected areas of Western Australia (Perth Basin). A report prepared for the Department of Industry and Resources, Western Australia. Geological Survey of Western Australia, Statutory petroleum exploration report, G31888 A2, unpublished.

Gibson, H., Bonet, C., Patterson, R., Seikel, R. and Hore, S. 2010. 3D Geological model building, and 3D temperature and heat flow calculation for the northern Perth Basin, A report prepared for Department of Mines and Petroleum by GeoIntrepid.. Geological Survey, Record 2011/6, 74pp.

Howard, L.E. and Sass, J.H. 1964. Terrestrial heat flow in Australia. Journal of Geophysical Research, 69, 1617-1626.

Lajaunie, Ch., Courrioux, G., and Manuel, L., 1997, Foliation fields and 3D cartography in geology: principles of a method based on potential interpolation: Mathematical Geology, 29, 571–584.

Middleton, M. F., 2010. The Gillingarra temperature anomaly, northern Perth Basin, Australia. 80th Annual Meeting of the Society of Exploration Geophysicists, Extended Abstracts.

Mory A. J., Haig D.W., McLoughlin S., and Hocking R. M., 2005, Geology of the northern Perth Basin, Western Australia – a field guide: Western Australia Geological Survey, Record 2005/9, 71p.

Mory A. J. and Iasky, R.P., 1996, Stratigraphy and structure of the onshore northern Perth Basin, Western Australia: Western Australia Geological Survey, Report 46.

Seikel, R., Stüwe K., Gibson H., Bendall B., McAllister L., Reid P., and Budd A., 2009, Forward prediction of spatial temperature variation from 3D geology models: 20th Australian Society of Exploration Geophysicists Conference, Extended Abstracts.

Stüwe, K., 2007, Geodynamics of the Lithosphere. An Introduction. 2nd Edition. Springer Verlag, 493p.